THE JOURNAL OF BIOLOGICAL CHEMISTRY
Vol. 279, No. 14, Issue of April 2, pp. 14184–14193, 2004
Printed in U.S.A.

pH Dependence and Stoichiometry of Binding to the Fc Region of IgG by the Herpes Simplex Virus Fc Receptor gE-gI*

Received for publication, December 5, 2003, and in revised form, January 14, 2004
Published, JBC Papers in Press, January 20, 2004, DOI 10.1074/jbc.M313281200

Elizabeth R. Sprague‡, W. Lance Martin‡§, and Pamela J. Bjorkman‡¶‖

From the ‡Division of Biology, ¶Howard Hughes Medical Institute, California Institute of Technology, Pasadena, California 91125

Herpes simplex virus type 1 encodes two glycoproteins, gE and gI, that form a heterodimer on the surface of virions and infected cells. The gE-gI heterodimer has been implicated in cell-to-cell spread of virus and is a receptor for the Fc fragment of IgG. Previous studies localized the gE-gI-binding site on human IgG to a region near the interface between the C_H2 and C_H3 domains of Fc, which also serves as the binding site for bacterial and mammalian Fc receptors. Although there are two potential gE-gI-binding sites per Fc homodimer, only one gE-gI heterodimer binds per IgG in gel filtration experiments. Here we report production of recombinant human Fc molecules that contain zero, one, or two potential gE-gI-binding sites and use them in analytical ultracentrifugation experiments to show that two gE-gI heterodimers can bind to each Fc. Further characterization of the gE-gI interaction with Fc reveals a sharp pH dependence of binding, with K_D values of ~340 and ~930 nM for the first and second binding events, respectively, at the slightly basic pH of the cell surface (pH 7.4), but undetectable binding at pH 6.0. This strongly pH-dependent interaction suggests a physiological role for gE-gI dissociation from IgG within acidic intracellular compartments, consistent with a mechanism whereby herpes simplex virus promotes intracellular degradation of anti-viral antibodies.

Alphaherpesviruses encode two glycoproteins that bind the Fc region of IgG to function together as a viral Fc receptor (FcR).[1] This FcR is a heterodimer composed of two type I transmembrane proteins, glycoprotein E (gE) and glycoprotein I (gI), on the surface of virions and virally infected cells (1–6). The herpes simplex virus type 1 (HSV-1) gE protein contains 550 amino acids, including an N-terminal hydrophobic leader sequence, an ~441-residue extracellular region followed by a predicted single transmembrane helix, and an ~106-residue C-terminal cytoplasmic tail. The HSV-1 gI protein contains 390 amino acids, including an N-terminal hydrophobic leader sequence, an ~248-amino acid extracellular portion followed by a predicted single transmembrane helix, and an ~94-amino acid C-terminal cytoplasmic tail. Potential endocytosis signals, including $YXX\phi$ motifs (tyrosine followed by any two amino acids and a hydrophobic residue), dileucine motifs, and acidic cluster motifs containing phosphorylation sites, are located in the cytoplasmic tails of gE and gI. Transfection experiments in HeLa cells to express HSV-1 gE proteins with truncated cytoplasmic tails localized two sorting signals: one located within an acidic stretch and a second located within a stretch of residues containing two tyrosine-based tetrapeptide motifs (7). These findings are consistent with studies of the gE cytoplasmic domains of two commonly studied alphaherpesviruses, pseudorabies virus (PRV) and varicella zoster virus (VZV), that identified functional roles for acidic motifs containing consensus casein kinase II phosphorylation sites and tyrosine motifs (8–12). A methionine-leucine endocytosis signal in the cytoplasmic tail of VZV gI has been shown to be important for the efficient internalization of gI in transfected HeLa cells (13).

In vitro and *in vivo* studies characterizing the FcR function of the gE-gI heterodimer have underscored its importance for alphaherpesviruses in escaping antibody-dependent components of the immune response. Mutational studies determined that the HSV-1 gE-gI heterodimer is required for high affinity binding of monomeric IgG, whereas gE alone is a monomeric, lower affinity FcR that only binds IgG-antigen immune complexes, such as IgG-coated erythrocytes (3, 14). FcR activity has also been demonstrated for gE-gI complexes from VZV and PRV (15, 16). The gE-gI complex may play a protective role whereby binding of the Fc portion of IgG could sterically inhibit neutralization of the virus or infected cells by anti-HSV antibodies as well as complement- and cell-mediated lysis of infected cells (17, 18). Additional data suggest that gE-gI binds anti-HSV IgG by a process known as antibody bipolar bridging in which the Fab domains of an anti-HSV antibody bind to specific viral antigens, and the Fc domain binds to gE-gI. FcR-mediated antibody bipolar bridging that interferes with antibody- and complement-mediated neutralization has been demonstrated on the surfaces of HSV-1 virions and virally infected cells (19). Furthermore, under conditions in which antibody bipolar bridging could occur, gE was required for the protection of infected cells from antibody-dependent cell-mediated cytotoxicity, C1q complement binding, and granulocyte attachment (20, 21). More recently, a functional HSV-1 FcR was shown to be critical for protecting HSV-1-infected mice from attack by human anti-HSV IgG (22).

Several properties of IgG binding by gE-gI have been elucidated. Early studies showed that IgG binding by HSV-1-infected cells is both species- and subtype-specific. Thus, rabbit

* This work was supported by a post-doctoral fellowship from the Leukemia and Lymphoma Society (to E. R. S.) and a Max Planck Research Award (to P. J. B.). The costs of publication of this article were defrayed in part by the payment of page charges. This article must therefore be hereby marked "*advertisement*" in accordance with 18 U.S.C. Section 1734 solely to indicate this fact.

§ Present address: Dept. of Biochemistry, Stanford University, Palo Alto, CA 94305.

‖ An Investigator of the Howard Hughes Medical Institute. To whom correspondence should be addressed. Tel.: 626-395-8350; Fax: 626-792-3683; E-mail: bjorkman@caltech.edu.

[1] The abbreviations used are: FcR, Fc receptor; bis-Tris, 2-[bis(2-hydroxyethyl)amino]-2-(hydroxymethyl)propane-1,3-diol; CHO, Chinese hamster ovary; gE, glycoprotein E; gI, glycoprotein I; hdFc, heterodimeric Fc; hIgG, human IgG; HSV-1, herpes simplex virus type 1; LDL, low density lipoprotein; MES, 4-morpholineethanesulfonic acid; MSX, methionine sulfoximine; nbFc, non-binding Fc; Ni-NTA, nickel-nitrilotriacetic acid; PRV, pseudorabies virus; RU, resonance unit; VZV, varicella zoster virus; wtFc, wild-type Fc.

IgG and human IgG (hIgG) subtypes 1, 2, and 4 (hIgG1, hIgG2, and hIgG4) bind to HSV-1, but rodent IgG and many allotypes of hIgG3 do not bind (23–27). Correlating with these results, the affinities of recombinant, soluble gE-gI for different hIgG subtypes derived from a surface plasmon resonance-based binding assay resulted in a rank ordering of the hIgG binding preference as follows: hIgG4 > hIgG1 ≥ hIgG2 (equilibrium dissociation constant (K_D) values ranging from 200 to 400 nM ⋙ hIgG3 (undetectable binding) (28). When the arginine at position 435 of hIgG3 was substituted with a histidine, which is the amino acid found at position 435 in hIgG1, hIgG2, and hIgG4, binding of gE-gI was partially restored (K_D ~1 μM), and conversely, when histidine 435 of hIgG4 was replaced with an arginine, binding was undetectable (28). These results suggest that the gE-gI-binding site on Fc includes residue 435 at the C_H2-C_H3 domain interface of Fc, consistent with the finding that fragment D of protein A, which also binds to the C_H2-C_H3 domain interface of Fc, inhibits binding of Fc fragments to HSV-1-infected cells (29).

In addition to gE-gI, other proteins known to recognize the C_H2-C_H3 domain interface of Fc regions of antibodies include bacterial FcRs (protein A and protein G), mammalian FcRs (FcαRI, a receptor for IgA, and FcRn, which transports IgG from the mother to the fetus or neonate), and rheumatoid factor, an autoimmune antibody that recognizes the Fc portion of IgG and IgM. Each of these Fc-binding proteins interacts with Fc at the C_H2-C_H3 domain junction of each subunit of the Fc dimer with a binding stoichiometry of two Fc-binding proteins per Fc molecule (30–36). Other FcRs, such as FcγRI, FcγRII, FcγRIII, and FcϵRI, mediate the interaction with their respective Fc partners via a portion of the C_H1-C_H2 hinge and a region of the C_H2 domain in an asymmetric interaction in which only one FcR binds to each Fc dimer (37–39). Although gE-gI shares an Fc-binding site with protein A, protein G, FcRn, and rheumatoid factor, our earlier characterization of the interaction between a soluble version of gE-gI and IgG suggested that only one gE-gI binds per IgG molecule (28). Because FcRn can form 1:1 complexes with IgG even though two FcRn molecules bind per IgG at equilibrium (40–42), we conducted additional experiments to investigate the binding stoichiometry of the gE-gI/Fc interaction. By using recombinant human Fc molecules that contain zero, one, or two potential gE-gI-binding sites, we determined the binding stoichiometry of gE-gI and Fc in an analytical ultracentrifugation assay. These experiments demonstrate that one or two gE-gI molecules can bind per Fc homodimer, analogous to other 2:1 FcR/Fc interactions in which the Fc-binding protein recognizes each of the C_H2-C_H3 domain interfaces on homodimeric Fc.

We also examined the binding of gE-gI to Fc as a function of pH, discovering that gE-gI binds tightly to Fc at neutral or slightly basic pH but undetectably at acidic pH. This pH-dependent Fc binding profile is opposite to that of FcRn, which exhibits a sharply pH-dependent binding profile with binding at acidic pH ≤ 6.5 but not at neutral pH (43–45). None of the other FcR/Fcγ interactions, however, are known to be affected by pH changes near neutral. The sharp pH dependence of the FcRn/Fc interaction is critical to its function by allowing FcRn to bind IgG in the acidic environment of intracellular transport vesicles and release IgG at the slightly basic pH of the bloodstream. We suggest that the opposite, but equally striking, pH-dependent binding properties of the gE-gI/Fc interaction play a role in gE-gI function, in the transport of anti-HSV antibodies from the cell surface to lysosomes for degradation.

EXPERIMENTAL PROCEDURES

Construction of and Expression of Soluble gE-gI and gE Vectors—A soluble version of the gE-gI heterodimer was expressed in CHO cells as described previously (28). Soluble gE-gI was also expressed in insect cells infected with a recombinant baculovirus encoding both gE and gI. For insect cell expression, standard PCR subcloning techniques were used to insert fragments of the gE (encoding residues 1–419) and gI (encoding residues 1–266) genes of HSV strain KOS into the BglII-EcoRI sites (gE) and BamHI site (gI) of the pAcUW51 dicistronic baculovirus expression vector (Pharmingen). An oligo-linker encoding a factor Xa cleavage site followed by six histidine residues and a stop codon was ligated into the vector in-frame with the 3′ end of the gI gene. An expression vector for gE alone with a C-terminal six-histidine tag was constructed by PCR subcloning a fragment of the gE gene of HSV strain KOS (encoding residues 1–390) into the BglII-EcoRI sites of pAcUW51 (Pharmingen) in-frame with an oligo-linker encoding a factor Xa cleavage site followed by six histidine residues and a stop codon at the 3′ end of the gE gene. The open reading frames of all constructs were completely sequenced. Recombinant baculovirus stocks for expression of gE-gI and gE were generated by cationic liposome cotransfection of the dicistronic expression plasmid with linear wild-type baculovirus DNA in High 5 insect cells (Invitrogen) as described by the manufacturer. The gI construct used in these experiments and in previous studies (28, 46) contains a deletion of residues 221–227, which comprise the last copy of a seven-amino acid repeat (*XXX*PSTT, where *X* is any amino acid) in the putative stalk region near the C terminus. The alteration in this region does not affect the Fc-binding function of the gE-gI heterodimer but significantly increases the expression levels of the heterodimer in insect cells, with the yield increasing from ~200 μg of purified gE-gI heterodimer per liter for expression of the unaltered construct to ~10 mg/liter for the altered construct (data not shown).

Purification of Soluble gE-gI Heterodimer—Soluble gE-gI was initially purified from either CHO cell supernatants directly or pH-adjusted insect cell supernatants by binding to an IgG affinity column (constructed by covalently coupling human IgG to Sepharose) at pH 7.4 and eluting at pH 11.5 as described (28). After the pH-dependent binding of gE-gI to Fc was discovered, we used a gentler protocol involving a pH 5.5 buffer (50 mM sodium citrate, 150 mM NaCl, 1 mM EDTA) to elute gE-gI from the IgG affinity column. Proteins eluted from the IgG affinity column were subsequently purified by size-exclusion chromatography on a Superdex 200 HR 10/30 or Superdex 200 HiLoad 16/60 column (Amersham Biosciences).

Purification of Soluble gE—Insect cell supernatants containing secreted gE were buffer exchanged into nickel-binding buffer (40 mM Tris, pH 8, 300 mM NaCl, 10 mM imidazole) and passed over a Ni-NTA-agarose column (Qiagen). Bound protein was eluted in buffer containing 40 mM Tris, pH 8, 300 mM NaCl, 250 mM imidazole and further purified by size-exclusion chromatography on a Superdex 75 HiLoad 26/60 column (Amersham Biosciences) that was equilibrated in 20 mM Tris, pH 7.8, 150 mM NaCl, 1 mM EDTA. Analysis of the peak fractions on a 12% SDS-PAGE gel showed a band migrating with an apparent molecular mass of 47 kDa (data not shown). Approximately 70 mg of gE were obtained per liter of insect cell supernatants.

Expression of Wild-type and Mutant Human Fc Proteins—Three forms of human Fc, wild-type Fc (wtFc), heterodimeric Fc (hdFc), and non-binding Fc (nbFc), which contain two, one, and zero potential gE-gI-binding sites, respectively, were constructed using a human IgG1 heavy chain cDNA (provided by David Cosman, Immunex, Seattle) as described previously for expression of the analogous forms of rat Fc (34). For expression of wild-type Fc, the DNA encoding the Fc region of human IgG1 (residues 223–447) was PCR-amplified and subcloned in-frame with the rat IgG2a signal sequence into pBJ5-GS, a mammalian expression vector that carries the glutamine synthetase gene as a means of selection and amplification in the presence of the drug methionine sulfoximine (MSX) (47). The expression vector encoding wtFc was transfected into CHO cells using the LipofectAMINE 2000 protocol (Invitrogen) with selection and amplification of stable cell lines using methionine sulfoximine as described (28, 43). Clones were screened for secretion of Fc by testing the supernatants for binding to protein A-Sepharose, as visualized on a Coomassie-stained 12% SDS-PAGE gel run under reducing and non-reducing conditions. Positive clones yielded a protein migrating with apparent molecular masses of 35 and 70 kDa under reducing and non-reducing conditions, respectively.

The nbFc expression construct was generated by mutating residues located in the vicinity of the C_H2-C_H3 domain interface of wtFc, a region of Fc that has been implicated in gE-gI binding (28). The QuikChange protocol (Stratagene) was used to make the following substitutions, which are analogous to substitutions introduced into rat Fc to abrogate binding to rat FcRn (34): Met-252 to Gly, Ile-253 to Gly, His-310 to Glu, His-433 to Glu, His-435 to Glu, and Tyr-436 to Ala. PCR was used to add a factor Xa cleavage site and six histidines to the 3′ end of the nbFc

construct. This DNA encoding nbFc was subcloned into pBJ5-GS as described above for wtFc. The expression vectors encoding wtFc and nbFc were cotransfected into CHO cells using the LipofectAMINE 2000 protocol (Invitrogen) with selection and amplification of stable cell lines using MSX as described (28, 43). Supernatants from clones that were viable in MSX were assayed for expression of either hdFc or nbFc by binding to Ni-NTA-agarose (Qiagen) and for expression of wtFc or hdFc by binding to FcRn-Sepharose, similar to the identification of clones expressing rat wtFc, hdFc, and nbFc (34). Positive clones secreted a mixture of hdFc, which is a heterodimer containing one wtFc and one nbFc chain, and wtFc and nbFc homodimers. On a 10% SDS-PAGE gel run under reducing conditions, nbFc migrates as a band of apparent molecular mass 37 kDa, wtFc migrates at an apparent molecular mass of 35 kDa, and hdFc migrates as two bands, 37 and 35 kDa (data not shown).

Purification of Human Fc Proteins—CHO cells were grown to confluence in 15-cm tissue culture plates, and supernatants were collected every 2–3 days. wtFc was purified from the harvest media using a modification of a previously described functional purification for rat Fc involving pH-dependent binding to a rat FcRn-Sepharose column (34). The pH of supernatants containing wtFc was adjusted to 5.8 with the addition of 1 M citrate buffer, pH 5.5 (~85 ml of citrate buffer/600 ml of supernatant), and then passed over the FcRn-Sepharose column. The column was washed with 50 mM citrate buffer, pH 5.5, 150 mM NaCl, 1 mM EDTA, 0.1% (w/v) NaN_3 and then eluted with 50 mM Tris, pH 8.3, 150 mM NaCl, 1 mM EDTA. Eluted proteins were concentrated in a 15-ml Amicon (10,000-Da cut-off) spin concentrator and either stored or loaded onto a Superdex 75 HR 10/30 or Superdex 75 HiLoad 16/60 column (Amersham Biosciences) that was equilibrated in 20 mM Hepes, pH 7.8, 150 mM NaCl. Peak fractions were concentrated to ~15 mg/ml and stored at 4 °C.

hdFc and nbFc were purified from media harvested from CHO cells that secrete a mixture of wtFc, hdFc, and nbFc. The purification scheme is similar to that used to purify rat hdFc and nbFc (34). In the first step, hdFc and nbFc are separated from wtFc using a Ni-NTA-agarose column (Qiagen) to which the double histidine tag of nbFc and the single histidine tag of hdFc bind. In the second step, hdFc and nbFc are separated at low pH by passage over an FcRn-Sepharose column, to which hdFc binds and nbFc flows through. Supernatants containing wtFc, hdFc, and nbFc were buffer exchanged into 40 mM Tris, pH 8, 300 mM NaCl, 10 mM imidazole, and 5% (w/v) glycerol and then mixed in batch with Ni-NTA-agarose. The Ni-NTA-agarose was washed with 40 mM Tris, pH 8, 300 mM NaCl, 10 mM imidazole and eluted with 40 mM Tris, pH 8, 300 mM NaCl, 250 mM imidazole. Peak fractions were collected, concentrated, and buffer exchanged in 50 mM citrate buffer, pH 5.5, 150 mM NaCl, 1 mM EDTA, and loaded onto a rat FcRn-Sepharose column. nbFc flows through this column, and hdFc was eluted at pH 8.3. To control for oversaturation of the FcRn column, the flow-through was passed over the column repeatedly until the final two passes showed no evidence of hdFc elution at pH 8.3. hdFc and nbFc were concentrated and buffer exchanged in 20 mM Hepes, pH 7.8, 150 mM NaCl, and then either stored or loaded onto a size-exclusion column as described for wtFc.

Protein concentrations were determined spectrophotometrically using extinction coefficients at 280 nm of 69,280 (wtFc, hdFc, and nbFc), 87,630 (gE-gI), and 64,010 M^{-1} cm^{-1} (gE), which were calculated from the amino acid sequence using the ProtParam tool in Expasy (48).

Analytical Ultracentrifugation—wtFc, hdFc, or nbFc were each mixed with insect cell-expressed gE-gI, which contains a C-terminal His_6 tag on gI, in various molar ratios from 1:1 (4.9 μM gE-gI, 4.9 μM Fc) to 6:1 (29.4 μM gE-gI, 4.9 μM Fc) in 20 mM Hepes, pH 7.8, 150 mM NaCl. Fc samples were examined alone at a concentration of 4.9 μM; gE-gI was examined alone at concentrations of 9.8 and 14.7 μM, and gE was examined alone at a concentration of 12 μM.

Sedimentation velocity experiments were carried out with two-sector charcoal-filled Epon 12-mm centerpieces equipped with quartz windows that were loaded with 416 μl of protein and 423 μl buffer as a reference. The samples were spun at 42,000 rpm at 20 °C in an An-60 Ti rotor in a Beckman Ultima XL-I analytical ultracentrifuge. Radial scans using absorbance optics were collected at 230, 250, or 280 nm with a step size of 0.003 cm in continuous mode at an interval of about 4 min until the samples reached the bottom of the cell. Data were analyzed using the *c*(*s*) routine in the program SEDFIT (49), which uses maximum entropy regularization and a finite element solution to the Lamm equation to fit the sedimentation data. The *c*(*s*) analysis results in a differential sedimentation coefficient distribution in which sample diffusion has been accounted for explicitly. The apparent sedimentation coefficients (*s**) reported in these studies were not corrected to standard conditions due to the complications of calculating partial specific volumes for the Fcs and gE-gI since they are glycosylated; however, all *s** values were determined under identical conditions. In the samples in which there was one predominant species, molecular masses were estimated using the fit value for the frictional ratio. The absorbance of samples used for centrifugation was measured at 230, 250, and 280 nm, and a scale factor between wavelengths was calculated for each set of samples with a given molar ratio. *c*(*s**) distributions were scaled such that all have units of A_{280} per Svedberg.

Biosensor Studies—Surface plasmon resonance studies were performed using a BIAcore 2000 instrument. Purified recombinant wtFc fragment in 10 mM sodium acetate, pH 4.6, was immobilized on a research-grade CM5 biosensor chip using primary amine coupling as described in the Biacore manual. For gE-gI binding to immobilized Fc, one flow cell was mock coupled with buffer only, whereas the other three flow cells were coupled with Fc at low coupling densities (75–467 resonance units (RU)) limiting the possibility of mass transport (50). Mass transport was not observed in a test in which gE-gI was injected at various flow rates, and the sensorgrams were superimposed to check whether or not the association phases aligned (data not shown). 3-Fold dilutions of a concentrated stock of purified CHO cell-expressed, soluble gE-gI were made starting at 10.9 μM and ending at 0.5 nM. For each binding experiment at a different pH, the pH of a triple buffer containing 25 mM sodium acetate, 25 mM MES, 25 mM bis-Tris propane, 150 mM NaCl, 3 mM EDTA, and 0.005% (v/v) P-20 surfactant was adjusted appropriately. 250 μl of each of the eight gE-gI concentrations and at least one buffer sample were injected at 50 μl/min, and RUs were recorded as a function of time. After the each injection of gE-gI, a 30-s injection of 250 mM di-ammonium hydrogen citrate, pH 5.0, was used to disrupt the binding and regenerate the surface.

Sensorgrams for the binding of gE-gI to immobilized wtFc at pH values between 6.0 and 8.2 in steps of 0.2 pH units were processed using the Scrubber software package (BioLogic Software, Campbell, Australia; www.biologic.com.au) and analyzed using single-site and bivalent ligand models in Clamp99 (51), a global fitting program that simultaneously fits the association and dissociation phases for all curves in a concentration set. The bivalent ligand model describes two sequential binding events for gE-gI binding to homodimeric Fc, yielding two sets of apparent on- and off-rate constants. Equilibrium dissociation constants (K_D) were calculated from the ratio of the apparent dissociation and association rate constants, yielding apparent K_D values for the first and second binding events ($K_{D1(app)}$ and $K_{D2(app)}$). The first apparent on-rate constant was converted to an intrinsic rate constant using a statistical factor to account for the two potential binding sites on Fc to which the first gE-gI molecule can bind, and the second apparent off-rate was converted to an intrinsic off-rate to account for the two sites on the fully bound complex from which the first dissociation event can occur. Thus, the intrinsic on-rate constant for the first gE-gI molecule is half that of the apparent rate constant ($k1_{on} = k1_{on(app)}/2$), and the intrinsic off-rate constant for the second molecule is half that of the apparent rate constant ($k2_{off} = k2_{off(app)}/2$). For independent binding sites, the calculated stepwise dissociation constants ($K_{D1(app)}$ and $K_{D2(app)}$) are related to the intrinsic binding constants for the first and second binding events to Fc (K_{D1} and K_{D2}) as shown in Equation 1,

$$K_{D1} = 2K_{D1(app)}$$
$$K_{D2} = K_{D2(app)}/2 \quad \text{(Eq. 1)}$$

Bulk refractive index and mass transport parameters were not fit, and curves with 2 RU or less binding were omitted from the fits. The quality of the fits for data generated at pH 6.2, 6.4, and 6.6 was improved by fixing the concentration parameter for Fc on the chip at the average value for the other pH values. Intrinsic equilibrium constants were plotted as equilibrium association constants (K_A), where $K_A = 1/K_D$, *versus* pH. Linear regression analysis was used to determine the slope of the best line through the data points between pH 6.4 and 7.0.

For gE binding to immobilized Fc, one flow cell was mock-coupled with buffer only, whereas the other three flow cells were coupled with wtFc, hdFc, or nbFc at densities between 200 and 600 RU. 2-Fold dilutions of a concentrated stock of purified, soluble gE were made starting at 105 μM and ending at 200 nM. 200 μl of each of the gE concentrations and at least two buffer samples were injected at 5 μl/min, and the RU was recorded as a function of time. Binding of gE to immobilized Fc was examined at pH 8.0 (50 mM Hepes, pH 8, 150 mM NaCl, 3 mM EDTA, and 0.005% (v/v) P-20 surfactant) and pH 6.0 (50 mM sodium phosphate buffer, pH 6, 150 mM NaCl, 3 mM EDTA, and 0.005% (v/v) P-20 surfactant), and sensorgrams were processed and analyzed

using the Scrubber software package (BioLogic Software Pty. Ltd., www.biologic.com.au). The K_D values were determined by plotting the response in the plateau region *versus* the logarithm of the analyte concentration for each concentration series and fitting the data to a single-site binding model.

RESULTS

Expression and Purification of gE-gI and Human Fc Proteins—Soluble gE-gI was produced and purified from the supernatants of transfected CHO cells or baculovirus-infected insect cells expressing the gE and gI ectodomains as described under the "Experimental Procedures" and Ref. 28. The resulting protein is a 1:1 gE-gI heterodimer composed of residues 21–399 of gE and residues 21–246 of gI (not including the hydrophobic leader sequences and transmembrane and cytoplasmic domains of both proteins) (28).

To investigate the interactions between gE-gI and IgG, we expressed mutant and wild-type forms of the Fc fragment of human IgG. Previous studies (28) with recombinant soluble gE-gI that compared the binding affinities for the human IgG subtypes showed that residue 435 at the C_H2-C_H3 domain interface within the Fc region of IgG is critical for gE-gI binding to IgG. We sought to define further the gE-gI interaction interface with IgG by constructing mutant Fc molecules in which residues in the putative gE-gI-binding site were mutated on one or both of the Fc subunits, analogous to previous studies of mutant rat Fc proteins used to investigate the rat FcRn/Fc interaction (34).

A wild-type Fc (wtFc) expression vector was constructed to express the Fc region of human IgG1. A nbFc construct was generated from the wtFc construct by mutating six residues located in the C_H2-C_H3 domain (Met-252 to Gly, Ile-253 to Gly, His-310 to Glu, His-433 to Glu, His-435 to Glu, and Tyr-436 to Ala) interface and adding a C-terminal His_6 tag. Four of the six residues that were substituted are part of a consensus binding site on Fc for protein A, protein G, rheumatoid factor, rat FcRn, and the Fc-III peptide (33, 52). Cotransfection of the wtFc and nbFc expression plasmids into CHO cells resulted in secretion of a mixture of wtFc homodimers, nbFc homodimers, and a hdFc that is composed of one wtFc chain and one nbFc chain. These three forms of human Fc were isolated from transfected cells as described previously for the wild-type, non-binding, and heterodimeric forms of rat Fc (34). Briefly, wtFc was purified from the supernatants of CHO cells that were transfected with only wtFc by taking advantage of its pH-dependent binding to FcRn. Thus, supernatants were passed over an FcRn-Sepharose column at pH 5.5 and eluted at pH 8.3. To obtain nbFc and hdFc, transfected CHO supernatants were passed over a Ni-NTA column, which binds the His-tagged Fcs (nbFc and hdFc). The eluant was then loaded onto the FcRn-Sepharose column at pH 5.5, which binds hdFc but not nbFc.

wtFc and hdFc, but Not nbFc, Bind to gE-gI—We used an analytical ultracentrifugation sedimentation velocity assay to compare the binding of purified gE-gI heterodimers to wtFc, hdFc, and nbFc. Data analyses were performed with the program SEDFIT using the $c(s)$ distribution of sedimentation coefficients, which allows for visualization of differentially sedimenting species as peaks in the distribution function (49). For each of the Fc molecules, the distribution of sedimentation coefficients was monitored in the presence and absence of gE-gI, with a change in the distribution indicating the formation of a new species. When equimolar concentrations of wtFc, hdFc, and nbFc were spun individually and their distribution functions were analyzed, each of the samples migrated with an apparent sedimentation coefficient (s^*) of 3.7 S with nearly overlapping distribution functions when the three samples were compared (Fig. 1*A*). These analyses show that the wtFc, hdFc, and nbFc proteins are dimers with the expected molecular masses that have similar hydrodynamic properties. The gE-gI alone sample had an s^* of 3.7 S and a small peak at 5.2 S that may be a small amount of aggregated gE-gI or an unidentified contaminant (Fig. 1*A*). Because the s^* values and peak profiles for the Fc proteins and gE-gI are virtually indistinguishable, only one peak that corresponds to both proteins would be observed in a mixture of gE and a non-binding version of Fc. Thus, when nbFc was mixed with gE-gI in various molar ratios, the s^* value of the major species remained constant at 3.7 S, and the distribution pattern did not change significantly (Fig. 1*B*). When hdFc was mixed with gE-gI in various molar ratios, the distribution function changed with the addition of gE-gI as indicated by the appearance of a new peak at 5.45 S (Fig. 1*C*). Likewise, sedimentation of the wtFc samples with gE-gI resulted in additional species with s^* values ranging from 5.6 to 6.55 S, depending on the wtFc:gE-gI molar ratio (Fig. 1*D*).

The change in the distribution of apparent sedimentation coefficients when hdFc and wtFc were mixed with gE-gI indicates that hdFc and wtFc bind gE-gI, whereas the lack of change in the distribution function when nbFc was mixed with gE-gI indicates that nbFc does not bind detectably to gE-gI. Thus, at least some of the residues in the C_H2-C_H3 domain interface that were mutated to make nbFc from wtFc contribute significantly to the binding surface with gE-gI. In addition, the ability of hdFc to bind gE-gI indicates that the gE-gI-binding site on Fc is contained primarily within a single wild-type Fc subunit rather than being composed of residues from both of the Fc subunits.

Two gE-gI Heterodimers Bind to Each wtFc—Sedimentation velocity centrifugation experiments were also performed to compare the stoichiometry of gE-gI binding to Fc molecules with two, one, or zero potential gE-gI-binding sites. Samples contained gE-gI and either wtFc, hdFc, or nbFc in molar ratios of 1:1, 2:1, 4:1, and 6:1 (gE-gI:Fc). The data were analyzed as described above. If the stoichiometry of gE-gI binding to Fc is 1:1, identical $c(s^*)$ distributions would be observed for wtFc and hdFc, independent of the concentration of gE-gI. If the stoichiometry of gE-gI binding to Fc is 2:1, new species with larger s^* values will appear as the molar ratio of gE-gI:wtFc is increased, eventually forming a saturated 2:1 gE-gI·wtFc complex, whereas the same species will be present for hdFc with all of the molar ratios. For the 1:1 sample containing hdFc and gE-gI, the majority of the sample sediments at 5.45 S. As the amount of gE-gI is increased and the concentration of hdFc remains fixed, the height and position of the peak at 5.45 S are constant, whereas the height of the peak at 3.7 S, which corresponds to excess gE-gI, increases (Fig. 1*C*). With wtFc and gE-gI, the species observed in the 1:1 sample migrates at 5.6 S, which is slightly larger than in the 1:1 hdFc sample, likely representing a mixture of primarily 1:1 complexes with some 2:1 complexes (Fig. 1*E*). As the amount of gE-gI is increased, the original peak at 5.6 S shifts to 6, 6.45, and 6.55 S in the 2:1, 4:1, and 6:1 samples, respectively, indicating that a new species is formed that saturates near the 4:1 input molar ratio (Fig. 1*D*). The increase in height of the 3.7 S peak as the molar ratio is increased from 2:1 to 4:1 and 6:1 indicates excess gE-gI, consistent with a 2:1 gE-gI/Fc stoichiometry. A comparison of the distribution of apparent sedimentation coefficients between samples containing nbFc, hdFc, and wtFc at each molar ratio tested is shown in Fig. 1, *E–H.* These data are consistent with a model whereby wtFc binds two molecules of gE-gI, one per Fc polypeptide chain, and hdFc binds only one molecule of gE-gI because it contains only a single potential gE-gI-binding site.

Biosensor Binding Experiments Support a Bivalent Binding Model—The binding properties for the interaction between

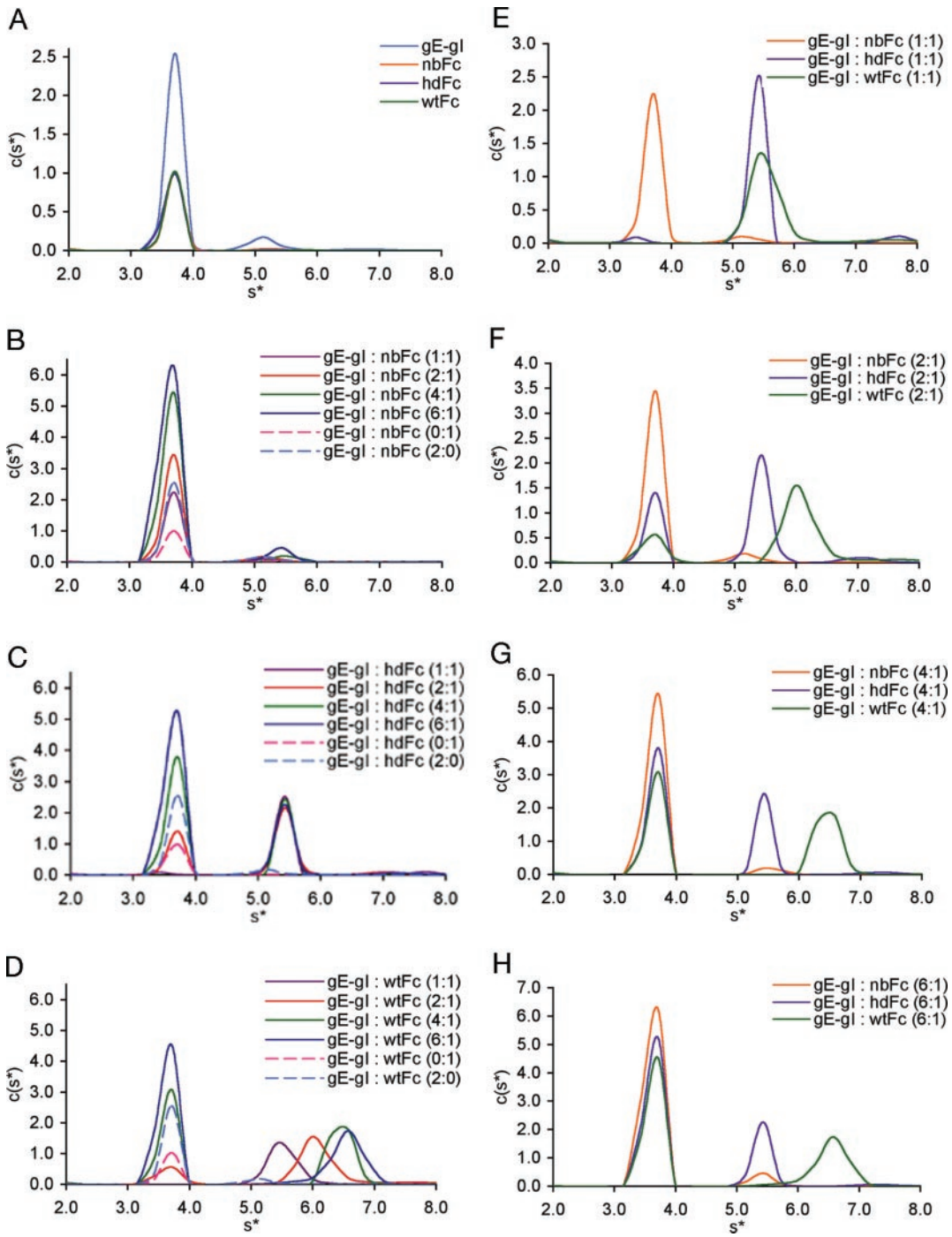

FIG. 1. **Binding of gE-gI to nbFc, hdFc, and wtFc as determined by sedimentation velocity.** Various concentrations of gE-gI were mixed with a fixed concentration of nbFc, hdFc, or wtFc at pH 7.8 and spun in an analytical ultracentrifuge. The distribution of apparent sedimentation coefficients ($c(s^*)$) in units of A_{280}/Svedberg is shown for each protein mixture. *A,* nbFc, hdFc, and wtFc alone and gE-gI alone (the three Fc species have nearly identical $c(s^*)$ distributions). *B,* 1:1, 2:1, 4:1, and 6:1 molar ratios of gE-gI with nbFc. *C,* 1:1, 2:1, 4:1, and 6:1 molar ratios of gE-gI with hdFc. *D,* 1:1, 2:1, 4:1, and 6:1 molar ratios of gE-gI with wtFc. *E,* 1:1 molar ratios of gE-gI with nbFc, hdFc, and wtFc. *F,* 2:1 molar ratios of gE-gI with nbFc, hdFc, and wtFc. *G,* 4:1 molar ratios of gE-gI with nbFc, hdFc, and wtFc. *H,* 6:1 molar ratios of gE-gI with nbFc, hdFc, and wtFc.

gE-gI and wtFc were further characterized by using a surface plasmon resonance assay. Recombinant wtFc (the "ligand") was immobilized at low coupling densities on the surface of a biosensor chip, and the binding of soluble gE-gI (the "analyte") was assayed at pH 7.4. Global fitting algorithms were used to fit the kinetic data to a single-site binding model from which a single equilibrium dissociation constant (K_D) is derived and to a bivalent ligand model that assumes that the wtFc ligand contains two independent binding sites for gE-gI, each of which can be described by a K_D value (K_{D1} and K_{D2}) (Fig. 2, *A* and *B*). The derived K_D value for gE-gI binding to wtFc assuming a single-site binding model was 340 nM, similar to previous surface plasmon resonance-based binding studies analyzing human IgG1 binding to immobilized gE-gI, in which the derived K_D value for a 1:1 binding model was ~280 nM (28). The present biosensor data for the interaction between soluble gE-gI and immobilized wtFc were better described by the bivalent ligand model than the single site model (Fig. 2, *A* and *B*), consistent with the analytical centrifugation studies demonstrating that gE-gI can bind to wtFc with a 2:1 binding stoichiometry (Fig. 1*D*). By using the bivalent ligand model, we determined K_D values of 343 nM (K_{D1}) and 928 nM (K_{D2}) for binding of gE-gI to

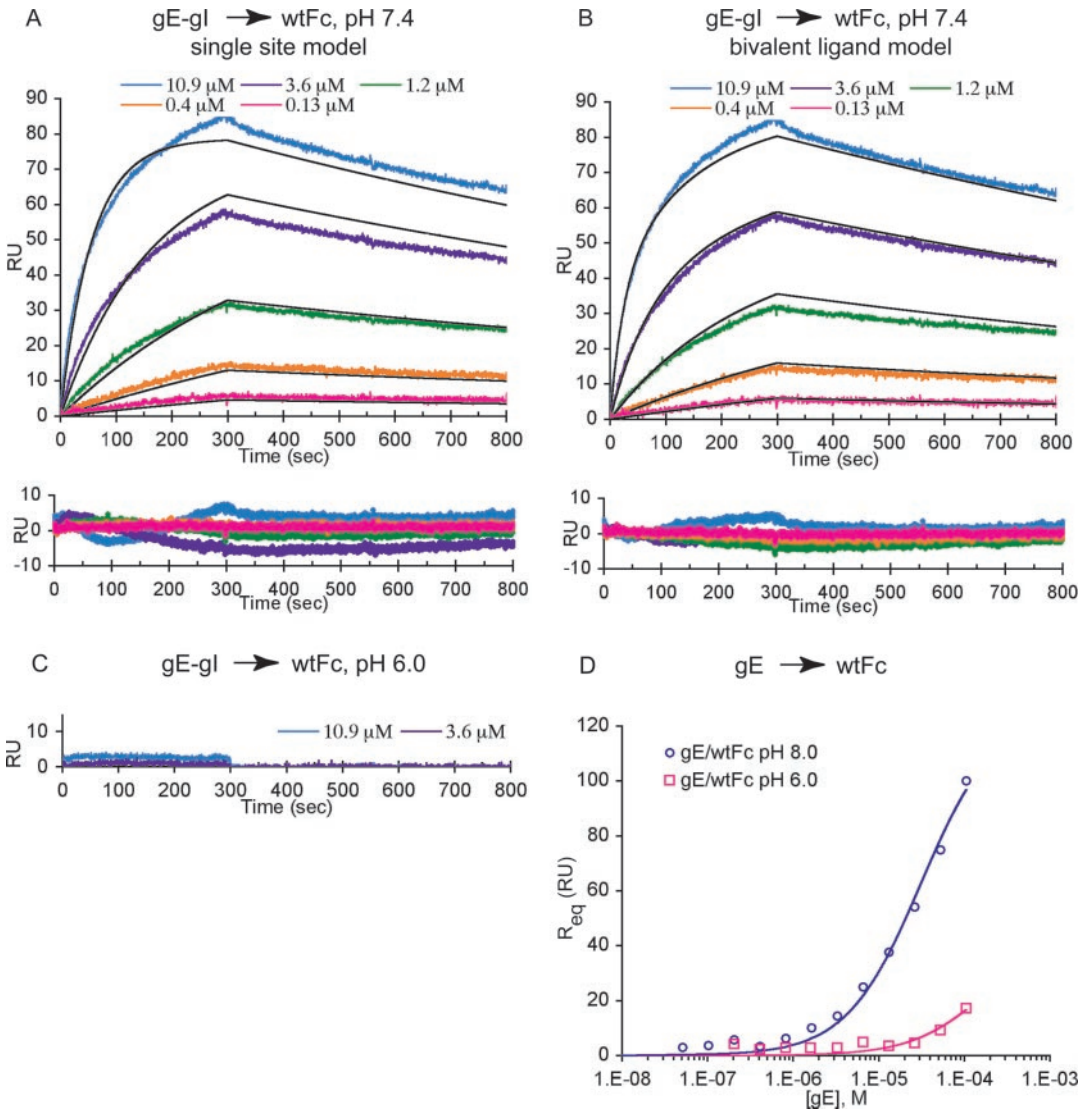

FIG. 2. **Biosensor analyses of gE-gI and gE binding to Fc.** Recombinant wtFc derived from human IgG1 was immobilized on the surface of a biosensor chip using primary amine coupling. *A* and *B,* comparison of fits (*thin black lines*) and associated residuals for sensorgrams (*thick colored lines*) collected from the indicated concentrations of gE-gI injected at pH 7.4 over a flow cell coupled with wtFc to 75 RU. *C,* sensorgrams collected from the indicated concentrations of gE-gI injected at pH 6.0 over a flow cell coupled with wtFc to 75RU. *D,* plot of equilibrium-binding response (R_{eq}) *versus* concentration of gE derived from biosensor experiments in which gE was injected at pH 8.0 and pH 6.0 over a flow cell coupled with wtFc. Best fit binding curves to the experimental data points are shown as *continuous lines.* Due to experimental limitations, data points at saturating concentrations of gE were unable to be obtained. Data collected at pH 8.0 are indicated in *blue circles*, and data collected at pH 6.0 are indicated in *pink squares.*

the first and the second binding sites on wtFc, respectively (Table I). Because the affinities of the two gE-gI-binding sites are similar, binding of one molecule of gE-gI does not significantly affect the binding of the second molecule. By using a single-site binding model for the interaction between immobilized hdFc and injected gE-gI, we derive a K_D of 447 nM (data not shown). Thus, the single gE-gI-binding site on hdFc has similar binding properties to each of the two gE-gI-binding sites on wtFc.

gE-gI and gE Bind Fc in a pH-dependent Manner—To investigate the possibility that gE-gI binding to Fc is pH-dependent, we conducted a series of surface plasmon resonance-based binding experiments at different pH values. Recombinant wtFc was immobilized on the surface of a biosensor chip; the binding of soluble gE-gI was assayed at different concentrations between pH values of 6.0 and 8.2 in 0.2 pH unit increments; and the binding data were fit to a bivalent ligand model (Table I). From pH 7.4 to 8.2, the K_D values (K_{D1} = 240–343 nM; K_{D2} = 669–928 nM) are relatively constant. At lower pH values, however, the affinities of the gE-gI interaction with wtFc decrease, dropping by 10-fold at pH 6.6 and becoming undetectable at pH 6.0 at concentrations up to 11 μM (Fig. 2*C*). The reduction in binding as the pH becomes more acidic is primarily the effect of an increased off-rate (Table I).

To estimate the number of ionizable residues involved in the pH-dependent affinity change observed for the gE-gI/Fc interaction, we plotted the equilibrium association constants (K_{A1} and K_{A2}) as a function of pH. The slope of the steepest section of this plot gives the net number of protons that are either released or taken up when gE-gI binds to wtFc over a given pH range. The slopes of the transitions between pH 6.4 and 7.0 are 2.1 and 2.2 for the first and second binding sites on wtFc, respectively, suggesting that two protons are released at each binding site on wtFc when gE-gI binds (Fig. 3). The steep transition in binding affinities suggests that the gE-gI/Fc binding interface involves two ionizable residues with pK_a values between pH 6.4 and 7.0. Histidines, which have a pK_a between 6 and 7 (53), are likely candidates for mediating pH-dependent

TABLE I

Comparison of the kinetic constants and binding affinities of the gE-gI·Fc complex at different pH values

Intrinsic kinetic and binding constants were converted from apparent constants determined from global fitting of the biosensor kinetic data to a bivalent ligand binding model as described under "Experimental Procedures."

pH	$k1_{off}$	$k1_{on}$	K_{D1}	$k2_{off}$	$k2_{on}$	K_{D2}
	s^{-1}	$M^{-1}\ s^{-1}$	nM	s^{-1}	$M^{-1}\ s^{-1}$	nM
8.2	5.0E−04	2.1E+03	240	3.6E−04	5.3E+02	676
8.0	5.1E−04	2.1E+03	246	3.6E−04	5.4E+02	669
7.8	5.1E−04	2.0E+03	261	3.7E−04	5.1E+02	732
7.6	5.6E−04	2.0E+03	283	4.2E−04	5.3E+02	796
7.4	6.3E−04	1.8E+03	343	4.8E−04	5.2E+02	928
7.2	7.9E−04	1.7E+03	474	6.2E−04	4.9E+02	1270
7.0	1.1E−03	1.5E+03	707	9.2E−04	4.8E+02	1910
6.8	1.7E−03	1.4E+03	1280	1.6E−03	4.9E+02	3330
6.6[a]	3.4E−03	1.0E+03	3300	4.9E−03	4.8E+02	10,200
6.4[a]	9.3E−03	7.4E+02	12600	1.9E−01	4.6E+03	41,200
6.2[b]	4.0E−02	1.1E+03	35700			
6.0[c]						

[a] Concentration of Fc was fixed during data analyses to improve the stability of the fits.
[b] Only one binding site was fit because fits allowing a second binding site were unstable.
[c] Kinetic constants could not be determined because the binding was too weak.

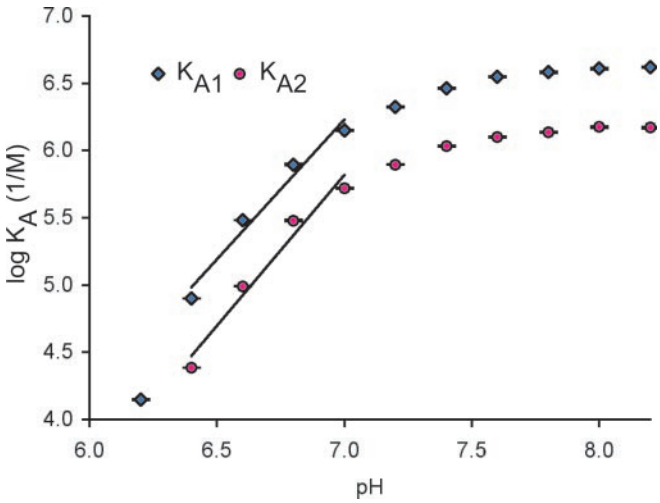

FIG. 3. **Analysis of the pH dependence of the gE-gI/Fc interaction.** K_{A1} (*blue diamonds*) and K_{A2} (*pink circles*) values were determined from kinetic analyses of surface plasmon resonance binding data collected at pH values between 6.0 and 8.2. The best fit line for points in the steepest portion of the pH-dependent affinity transition (pH 6.4, 6.6, 6.8, and 7.0) is shown for the intrinsic K_{A1} (corresponding to the first gE-gI binding to Fc) and K_{A2} (corresponding to the second gE-gI binding to Fc) values. The slopes for the lines are 2.1 and 2.2 for the first and second binding sites, respectively.

interactions near neutral pH. At basic pH, where gE-gI binds the Fc of IgG, histidines are uncharged, whereas at acidic pH, histidines are protonated and positively charged. One mechanism to explain the pH-dependent interaction between gE-gI and Fc is that the interface between gE-gI and Fc contains two histidines that disrupt hydrophobic contacts or contacts with a positively charged residue when protonated at acidic pH. Although our analysis does not allow insight into which binding partner contains the two ionizable residues, it is tempting to speculate that Fc His-435 and perhaps one of the other conserved histidines at the C_H2-C_H3 interface (His-310 or His-433) are involved in the pH-dependent interaction with gE-gI. Alternatively, conserved histidines in gE and/or gI may also be involved.

To further characterize the pH dependence of the gE-gI interaction with Fc, we tested whether isolated gE monomers bind to Fc with pH dependence using the surface plasmon resonance assay. Because the on- and off-rates for the gE/Fc interaction are too fast to obtain useful kinetic data (data not shown), the binding affinity was determined using an equilibrium-binding method. Although Fc contains two potential binding sites for gE, a single-site model was used to fit the data because the binding was too weak to allow accurate fitting of a two-site model. At pH 8, the derived K_D was ~30 μM, which is ~100-fold weaker than the gE-gI/Fc interaction (Fig. 2*D*), consistent with previous characterizations of gE alone as a low affinity FcR that binds IgG-antigen immune complexes but not isolated IgG (3, 14). Similar to the gE-gI/Fc interaction, the gE/Fc interaction is pH-dependent with binding becoming too weak to calculate a K_D at pH 6 (Fig. 2*D*). Thus, the pH dependence of the gE-gI interaction with IgG is likely to involve residues on gE and/or Fc.

DISCUSSION

The herpesvirus gE-gI heterodimer is found on the surface of virions and infected cells and binds the Fc region of IgG (1–6). Previous surface plasmon resonance assays of the interaction between soluble gE-gI and hIgG revealed that gE-gI binds to the hIgG1, hIgG2, and hIgG4 subclasses with affinities ~300 nM but does not show detectable binding to hIgG3 at concentrations up to 3 μM (28), consistent with IgG binding studies using HSV-1-infected cells (24, 26, 27). The previous biosensor study also identified residue 435, located in the Fc region of the IgG heavy chain, as a critical residue for IgG binding by gE-gI (28), consistent with the observation that a proteolytic fragment of protein A, which binds to the C_H2-C_H3 domain interface of Fc containing His-435, inhibited the binding of Fc fragments to HSV-infected cells (29). Here we use a soluble version of gE-gI and recombinant Fc molecules containing zero, one, or two potential gE-gI-binding sites to further characterize the Fc binding properties of gE-gI. The mutant Fc molecules were made by altering six of the residues in the C_H2-C_H3 domain interface of human Fc in either one or both of the Fc chains. Four of the six residues that were mutated mediate specific, yet diverse, interactions in the Fc binding interfaces for protein A, protein G, rheumatoid factor, and FcRn (30–33), as well as Fc-III, a high affinity Fc-binding peptide that was identified in a phage display assay (52). In a sedimentation velocity centrifugation assay, both wtFc and hdFc, which is a Fc molecule containing one copy of the mutant subunit and one copy of the wild-type subunit, bind gE-gI. gE-gI did not bind to nbFc, which is a homodimeric Fc containing two copies of the mutant subunit. These data confirm the importance of the C_H2-C_H3 domain interface of Fc in binding of gE-gI. Furthermore, they imply that the gE-gI-binding site is contained, at least primarily, within a single Fc subunit, unlike the mammalian FcRγ receptors, which recognize a single binding site on Fc composed

of residues contributed by both Fc subunits (37).

To date all of the proteins whose contacts with Fc are mediated through the C_H2-C_H3 domain interface can form 2:1 complexes with Fc, with one molecule binding to each Fc subunit. Our previous experiments using non-equilibrium and equilibrium gel filtration assays suggested that gE-gI forms 1:1 complexes with IgG (28). Using three recombinant Fc molecules (wtFc, hdFc, and nbFc) in a more sensitive assay involving analytical ultracentrifugation, we show that gE-gI can form 2:1 complexes with wtFc and only 1:1 complexes with hdFc. The data are also consistent with the formation of both 1:1 and 2:1 (gE-gI·wtFc) complexes under non-saturating conditions of gE-gI. Furthermore, surface plasmon resonance-based assays with gE-gI and Fc support a bivalent ligand model with K_D values of 343 and 928 nM for the first and second binding sites on wtFc, respectively.

The finding that each chain of the Fc homodimer has a binding site of similar affinity for the gE-gI heterodimer may allow for antibody-mediated cross-linking of gE-gI proteins on the surface of infected cells. Such cross-linking would involve two gE-gI molecules bridged by IgG or, in the case of antibody bipolar bridging, two gE-gI molecules bridged by IgG bound to HSV antigens (*e.g.* gB or gD) via the antibody Fab arms. Antibody bipolar bridging between gE-gI and surface antigens involving 1:1 gE-gI·IgG complexes might still trigger the host complement cascade through interactions of one of the C_H2 domains of Fc with C1q. By contrast, in a 2:1 gE-gI·IgG complex in which each Fc chain interacts with a gE-gI molecule, the binding of C1q is more likely to be sterically hindered, thus preventing initiation of the complement cascade. Likewise, 2:1 gE-gI·IgG complexes may be less accessible than 1:1 complexes for interactions with host Fc receptors, such as FcγRI, FcγRII, and FcγRIII. Thus, formation of 2:1 complexes may enhance the immune evasion effects that have been observed in the presence of antibody bipolar bridging (19–22). The ability of gE-gI to form either 1:1 or 2:1 complexes with IgG may be related to the amount of gE-gI on the cell surface compared with the amount of available IgG. The concentration of IgG in the serum is ~10-fold higher than the K_D values for binding gE-gI, thereby predicting that gE-gI would form primarily 1:1 complexes with free IgG. Anti-HSV IgG that is sequestered at the cell surface through antigen recognition by the Fabs, however, would be present at a much lower concentration, allowing for formation of 2:1 complexes with gE-gI. This potential difference in receptor:IgG stoichiometry provides a mechanism by which an HSV-infected cell can distinguish between nonimmune IgG and anti-HSV IgG. The gE-gI cytoplasmic tails, which contain potential signaling motifs including tyrosine-based tetrapeptide motifs, dileucine motifs, and phosphorylation sites (7–13), are predicted to be arranged differently for 2:1 *versus* 1:1 complexes, resulting in a different set of downstream effects. For example, in the case of 2:1, but not 1:1, complexes, the cytoplasmic tails of cross-linked gE-gI molecules may be in position to interact with each other or another protein.

Previous studies (28, 29) and the data reported here localize the gE-gI-binding site to the C_H2-C_H3 domain interface of Fc, a site that is recognized by a number of other Fc receptors including FcRn, which binds to IgG with sharp pH dependence. FcRn binds IgG in the acidic environment of intracellular vesicles or the lumen of the gut and releases it at the cell surface (pH 7.4) (54–56). The sharp pH dependence of the rat FcRn/rat Fc interaction has been attributed to three pairs of titrating salt bridges in the binding interface, each involving an Fc histidine and an acidic FcRn residue (Fc His-310/FcRn Glu-117, Fc His-435/FcRn Glu-132, and Fc His-436/FcRn Asp-137) (33, 45, 57–59). The Fc histidines are protonated under acidic conditions, forming salt bridges with the negatively charged residues on FcRn, which are disrupted upon deprotonation of the histidines at neutral and basic pH, thereby leading to dissociation of Fc from FcRn (33). His-435, which is involved in the pH modulation of the rat FcRn-rat Fc complex, is conserved in the human IgG subclasses hIgG1, hIgG2, and hIgG4, and is also found in the common binding site at the C_H2-C_H3 domain interface that has been described for many Fc-binding proteins (33, 52). Although His-435 is an important contact residue for Fc binding to protein A, protein G, and rheumatoid factor (30–32), none of the interactions of these proteins with Fc are sharply affected by changes of pH near neutral. Here we report the unexpected result that the binding of Fc to the viral FcR gE-gI is tightly pH-regulated, with the highest affinity at the slightly basic pH of the extracellular milieu and undetectable binding at the acidic pH of endosomes. At pH values between 7.4 and 8.2 the affinities of the two gE-gI-binding sites are similar ($K_D1 \approx 240$–340 nM and $K_D2 \approx 670$–930 nM); however, as the pH is decreased, the affinities become weaker until no binding is detectable at pH 6.0 at concentrations up to 11 μM. An analysis of the pH-dependent affinity transition for the gE-gI/Fc interaction suggests that two ionizable residues that become protonated between pH 6.4 and 7.0 modulate this sharply pH-dependent interaction. Because histidine residues have a pK_a near neutral pH, Fc His-435 could be involved in the pH-dependent affinity transition. Although residues on gI must affect Fc binding because gE-gI binds 100-fold more tightly to Fc than gE alone, the finding that binding of isolated gE to Fc is also pH-dependent suggests that at least some of the pH dependence of the gE-gI interaction with Fc resides in gE and/or Fc.

Mechanistic details for how a small change in pH modulates the gE-gI/Fc interaction are unclear, but the present data allow us to address some potential mechanisms. The possibility that gE-gI itself dissociates at acidic pH as a result of a chemical change at the interface of the gE-gI heterodimer is unlikely because analytical ultracentrifugation results demonstrate that the gE-gI heterodimer remains intact at acidic pH values similar to intracellular endosomes. At pH 6, s^* values of 3.45 S for gE-gI and 2.6 S for gE were measured (data not shown). These data are consistent with internalization experiments in which the gE-gI complex was precipitated with an antibody to either gE or gI (13). Another possible explanation for the pH dependence of the gE-gI/Fc interaction is a change at the gE-gI/Fc interface, either conformational or chemical, that disrupts the interaction at acidic pH. Conformational changes in Fc are unlikely since a comparison of the structures of Fc molecules that have been solved at pH values between 4.1 and 8.0 revealed no significant differences (30–33, 37, 52, 60). Thus, it is likely that the pH-dependent interaction between gE-gI and Fc results either from chemical changes in Fc and/or chemical or conformational changes in gE-gI. The small difference in the sedimentation coefficient of gE-gI at pH 7.8 *versus* pH 6.0 (3.7 S at pH 7.8; 3.45 S at pH 6.0) suggests the possibility of a pH-dependent conformational change in gE-gI. Further structural, biophysical, and mutational analyses of gE-gI and the gE-gI interaction with Fc will be required to elucidate the mechanism by which gE-gI discriminates between Fc at acidic and basic pH values.

The sharply pH-dependent affinity transition near neutral pH of the gE-gI interaction with the Fc region of IgG is an unusual feature of a protein/protein interaction, implying a functional significance that could involve receptor-mediated endocytosis. Receptor-mediated endocytosis is a process by which receptors transport ligands (*e.g.* small molecules or proteins) between the intracellular and extracellular environ-

ments, often taking advantage of the differences in pH between the cell surface and intracellular vesicles to regulate the process (61). In addition to gE-gI/IgG, receptor-ligand pairs demonstrating similarly strong pH-dependent interactions near neutral pH include FcRn and IgG (tight binding at acidic but not basic pH), apotransferrin and transferrin receptor (tight binding at acidic but not basic pH), and low density lipoprotein (LDL) and its receptor (LDL receptor) (tight binding at basic but not acidic pH). In each case, the pH-dependent receptor/ligand interaction is critical for a function in intracellular trafficking, such that the receptor-ligand complex either forms or dissociates only at the slightly basic pH of the extracellular milieu or inside acidic intracellular vesicles. For example, FcRn and transferrin receptor only bind to their IgG or apotransferrin ligands in the acidic environment of endosomes and then release their ligands upon exposure to the bloodstream (54–56, 62). Conversely, LDL binds its receptor at the cell surface and then is released in acidic endosomes so that LDL receptor can be recycled and LDL is targeted for degradation in lysosomes (63). The gE-gI interaction with IgG shows the same trend in pH-dependent binding as the interaction between LDL and LDL receptor, suggesting a similar trafficking mechanism whereby gE-gI·IgG complexes are endocytosed from the cell surface to enter acidic endosomes where IgG dissociates from gE-gI and is then degraded in lysosomes.

In support of our proposal of receptor-mediated endocytosis of IgG by gE-gI, several studies have investigated the endocytosis of gE, gI, and gE-gI. Experiments using transfected and/or infected cells demonstrated that the gE proteins of HSV, PRV, and VZV and the gI proteins of VZV and PRV undergo endocytosis (7–10, 12, 13, 64–66). Furthermore, the colocalization of VZV gE with transferrin receptor during endocytosis and recycling in transfected cells suggests that gE travels from the plasma membrane to the early endosomes and then is recycled back to the cell surface (9). When both VZV gE and gI are expressed in HeLa cells, gE and gI colocalize during endocytosis and recycling with evidence from quantitative internalization assays suggesting that gE and gI are internalized as a complex (13). Additional experiments support the suggestion that gE and/or gE-gI heterodimers function in receptor-mediated endocytosis of IgG followed by its degradation. VZV gE-expressing HeLa cells bind IgG Fc at the cell surface, which becomes undetectable both inside and outside the cells upon incubation at 37 °C, consistent with intracellular degradation (9). Although internalization of gE or the gE-gI complex has not been shown to be dependent on antibody binding via Fc with or without antibody bipolar bridging, it is possible that antibody binding affects the endocytosis of these molecules by increasing the efficiency or kinetics of internalization, for example.

There are several possibilities for how gE-gI-mediated endocytosis of anti-HSV antibodies could facilitate immune evasion by HSV. Binding of an anti-HSV antibody via its Fab arms to an HSV antigen and via its Fc domain to gE-gI might induce internalization of the entire gE-gI·IgG·antigen complex, thereby removing HSV antigens from the cell surface and thus reducing antibody-mediated immune responses such as antibody-dependent cell-mediated cytotoxicity or antibody-dependent complement-mediated lysis. In PRV-infected monocytes, incubation with anti-PRV antibodies resulted in the aggregation and internalization of many cell surface proteins and in the inhibition of antibody-dependent complement-mediated lysis, which was dependent on IgG binding by PRV gE-gI (67, 68). The finding that HSV-1 gE-gI binding of IgG is pH-dependent strongly suggests another hypothesis for how endocytosis of gE-gI-antibody complexes hinders the host immune response, namely that IgG molecules and IgG-antigen complexes brought into acidic compartments by gE-gI are targeted for degradation in lysosomes after low pH-induced dissociation from gE-gI, thereby reducing the ability of the host to mount antibody-dependent immune responses and to make immune responses to viral antigens.

Acknowledgments—We thank Inder Nangiana, Cynthia Jones, and Peter Snow (Caltech Protein Expression Facility) for insect cell expression of gE-gI and gE; Noreen Tiangco for CHO cell expression of hdFc and nbFc; Anthony West, Anthony Giannetti, and Andrew Herr for advice on biosensor and analytical ultracentrifugation experiments; and Malini Raghavan and members of the Bjorkman laboratory for critical reading of the manuscript.

REFERENCES

1. Westmoreland, D., and Watkins, J. F. (1974) *J. Gen. Virol.* **24,** 167–178
2. Johnson, D. C., and Feenstra, V. (1987) *J. Virol.* **61,** 2208–2216
3. Johnson, D. C., Frame, M. C., Ligas, M. W., Cross, A. M., and Stow, N. D. (1988) *J. Virol.* **62,** 1347–1354
4. Whitbeck, J. C., Knapp, A. C., Enquist, L. W., Lawrence, W. C., and Bello, L. J. (1996) *J. Virol.* **70,** 7878–7884
5. Yao, Z., Jackson, W., Forghani, B., and Grose, C. (1993) *J. Virol.* **67,** 305–314
6. Zuckermann, F. A., Mettenleiter, T. C., Schreurs, C., Sugg, N., and Ben-Porat, T. (1988) *J. Virol.* **62,** 4622–4626
7. Alconada, A., Bauer, U., Sodeik, B., and Hoflack, B. (1999) *J. Virol.* **73,** 377–387
8. Zhu, Z., Hao, Y., Gershon, M. D., Ambron, R. T., and Gershon, A. A. (1996) *J. Virol.* **70,** 6563–6575
9. Olson, J. K., and Grose, C. (1997) *J. Virol.* **71,** 4042–4054
10. Alconada, A., Bauer, U., and Hoflack, B. (1996) *EMBO J.* **15,** 6096–6110
11. Olson, J. K., Bishop, G. A., and Grose, C. (1997) *J. Virol.* **71,** 110–119
12. Tirabassi, R. S., and Enquist, L. W. (1999) *J. Virol.* **73,** 2717–2728
13. Olson, J. K., and Grose, C. (1998) *J. Virol.* **72,** 1542–1551
14. Dubin, G., Frank, I., and Friedman, H. M. (1990) *J. Virol.* **64,** 2725–2731
15. Litwin, V., Jackson, W., and Grose, C. (1992) *J. Virol.* **66,** 3643–3651
16. Favoreel, H. W., Nauwynck, H. J., Van Oostveldt, P., Mettenleiter, T. C., and Pensaert, M. B. (1997) *J. Virol.* **71,** 8254–8261
17. Adler, R., Glorioso, J. C., Cossman, J., and Levine, M. (1978) *Infect. Immun.* **21,** 442–447
18. Dowler, K. W., and Veltri, R. W. (1984) *J. Med. Virol.* **13,** 251–259
19. Frank, I., and Friedman, H. M. (1989) *J. Virol.* **63,** 4479–4488
20. Dubin, G., Socolof, E., Frank, I., and Friedman, H. M. (1991) *J. Virol.* **65,** 7046–7050
21. Van Vliet, K. E., De Graaf-Miltenburg, L. A., Verhoef, J., and Van Strijp, J. A. (1992) *Immunology* **77,** 109–115
22. Nagashunmugam, T., Lubinski, J., Wang, L., Goldstein, L. T., Weeks, B. S., Sundaresan, P., Kang, E. H., Dubin, G., and Friedman, H. M. (1998) *J. Virol.* **72,** 5351–5359
23. Johansson, P. J., Hallberg, T., Oxelius, V. A., Grubb, A., and Blomberg, J. (1984) *J. Virol.* **50,** 796–804
24. Johansson, P. J., Myhre, E. B., and Blomberg, J. (1985) *J. Virol.* **56,** 489–494
25. Johansson, P. J., Schroder, A. K., Nardella, F. A., Mannik, M., and Christensen, P. (1986) *Immunology* **58,** 251–255
26. Johansson, P. J., Ota, T., Tsuchiya, N., Malone, C. C., and Williams, R. C., Jr. (1994) *Immunology* **83,** 631–638
27. Wiger, D., and Michaelsen, T. E. (1985) *Immunology* **54,** 565–572
28. Chapman, T. L., You, I., Joseph, I. M., Bjorkman, P. J., Morrison, S. L., and Raghavan, M. (1999) *J. Biol. Chem.* **274,** 6911–6919
29. Johansson, P. J. H., Nardella, F. A., Sjoquist, J., Schroder, A. K., and Christensen, P. (1989) *Immunology* **66,** 8–13
30. Sauer-Eriksson, A. E., Kleywegt, G. J., Uhlen, M., and Jones, T. A. (1995) *Structure* **3,** 265–278
31. Corper, A. L., Sohi, M. K., Bonagura, V. R., Steinitz, M., Jefferis, R., Feinstein, A., Beale, D., Taussig, M. J., and Sutton, B. J. (1997) *Nat. Struct. Biol.* **4,** 374–381
32. Deisenhofer, J. (1981) *Biochemistry* **20,** 2361–2370
33. Martin, W. L., West, A. P., Jr., Gan, L., and Bjorkman, P. J. (2001) *Mol. Cell* **7,** 867–877
34. Martin, W. L., and Bjorkman, P. J. (1999) *Biochemistry* **38,** 12639–12647
35. Herr, A. B., Ballister, E. R., and Bjorkman, P. J. (2003) *Nature* **423,** 614–620
36. Herr, A. B., White, C. L., Milburn, C., Wu, C., and Bjorkman, P. J. (2003) *J. Mol. Biol.* **327,** 645–657
37. Sondermann, P., Huber, R., Oosthuizen, V., and Jacob, U. (2000) *Nature* **406,** 267–273
38. Garman, S. C., Wurzburg, B. A., Tarchevskaya, S. S., Kinet, J. P., and Jardetzky, T. S. (2000) *Nature* **406,** 259–266
39. Ghirlando, R., Keown, M. B., Mackay, G. A., Lewis, M. S., Unkeless, J. C., and Gould, H. J. (1995) *Biochemistry* **34,** 13320–13327
40. Huber, A. H., Kelley, R. F., Gastinel, L. N., and Bjorkman, P. J. (1993) *J. Mol. Biol.* **230,** 1077–1083
41. Popov, S., Hubbard, J. G., Kim, J., Ober, B., Ghetie, V., and Ward, E. S. (1996) *Mol. Immunol.* **33,** 521–530
42. Sanchez, L. M., Penny, D. M., and Bjorkman, P. J. (1999) *Biochemistry* **38,** 9471–9476
43. Gastinel, L. N., Simister, N. E., and Bjorkman, P. J. (1992) *Proc. Natl. Acad. Sci. U. S. A.* **89,** 638–642
44. Simister, N. E., and Mostov, K. E. (1989) *Cold Spring Harbor Symp. Quant. Biol.* **54,** 571–580
45. Simister, N. E., and Mostov, K. E. (1989) *Nature* **337,** 184–187
46. Rizvi, S. M., and Raghavan, M. (2001) *J. Virol.* **75,** 11897–11901

47. Bebbington, C. R., and Hentschel, C. C. G. (1987) in *DNA Cloning: A Practical Approach* (Glover, D. M., ed) pp. 163–188, IRL Press at Oxford University Press, Oxford
48. Gill, S. C., and von Hippel, P. H. (1989) *Anal. Biochem.* **182,** 319–326
49. Schuck, P. (2000) *Biophys. J.* **78,** 1606–1619
50. Karlsson, R., and Falt, A. (1997) *J. Immunol. Methods* **200,** 121–133
51. Morton, T. A., and Myszka, D. G. (1998) *Methods Enzymol.* **295,** 268–294
52. DeLano, W. L., Ultsch, M. H., de Vos, A. M., and Wells, J. A. (2000) *Science* **287,** 1279–1283
53. Stryer, L. (1988) *Biochemistry*, 3rd Ed., p. 21, W. H. Freeman & Co., New York
54. Junghans, R. P. (1997) *Immunol. Res.* **16,** 29–57
55. Ghetie, V., and Ward, E. S. (1997) *Immunol. Today* **18,** 592–598
56. Simister, N. E., Jacobowitz Israel, E., Ahouse, J. C., and Story, C. M. (1997) *Biochem. Soc. Trans.* **25,** 481–486
57. Ghetie, V., and Ward, E. S. (2000) *Annu. Rev. Immunol.* **18,** 739–766
58. Raghavan, M., Bonagura, V. R., Morrison, S. L., and Bjorkman, P. J. (1995) *Biochemistry* **34,** 14649–14657
59. Vaughn, D. E., Milburn, C. M., Penny, D. M., Martin, W. L., Johnson, J. L., and Bjorkman, P. J. (1997) *J. Mol. Biol.* **274,** 597–607
60. Harris, L. J., Larson, S. B., Hasel, K. W., and McPherson, A. (1997) *Biochemistry* **36,** 1581–1597
61. Mellman, I. (1996) *Annu. Rev. Cell Dev. Biol.* **12,** 575–625
62. de Silva, D. M., Askwith, C. C., and Kaplan, J. (1996) *Physiol. Rev.* **76,** 31–47
63. Brown, V. I., and Greene, M. I. (1991) *DNA Cell Biol.* **10,** 399–409
64. Tirabassi, R. S., and Enquist, L. W. (1998) *J. Virol.* **72,** 4571–4579
65. Pasieka, T. J., Maresova, L., and Grose, C. (2003) *J. Virol.* **77,** 4191–4204
66. Zhu, Z., Gershon, M. D., Hao, Y., Ambron, R. T., Gabel, C. A., and Gershon, A. A. (1995) *J. Virol.* **69,** 7951–7959
67. Van de Walle, G. R., Favoreel, H. W., Nauwynck, H. J., and Pensaert, M. B. (2003) *J. Gen. Virol.* **84,** 939–948
68. Favoreel, H. W., Nauwynck, H. J., Van Oostveldt, P., and Pensaert, M. B. (2000) *Virology* **267,** 151–158